EAI Endorsed Transactions
on Industrial Networks and Intelligent Systems
Research Article EAI.EU

Constellation Design for Blind Detection of Orthogonal Space–Time Block Codes in Wireless MIMO Systems

Minh-Tuan Le*, Trung-Hieu Nguyen

Faculty of Electronics Engineering 1, Posts and Telecommunications Institute of Technology (PTIT), Hanoi, Vietnam

Abstract

This paper investigates the problem of blind detection of orthogonal space–time block codes (OSTBCs) with quadrature amplitude modulation (QAM) in multiple-input multiple-output (MIMO) systems over quasi-static flat Rayleigh fading channels. To resolve the inherent rotational ambiguity in blind OSTBC detection, we propose a structurally constrained QAM constellation that enables unique symbol recovery without the use of pilot signals. Building on this design, we develop a low-complexity iterative detector, referred to as the iterative maximum-likelihood with averaged initial channel estimate (IML-AICE) detector, which jointly estimates the channel and transmitted symbols. The proposed detector incorporates a novel initialization strategy and an iterative refinement mechanism inspired by clairvoyant maximum-likelihood detection, leading to improved convergence and detection accuracy. The proposed framework enables reliable blind recovery of OSTBC symbols, thereby improving spectral efficiency by eliminating pilot overhead. Simulation results demonstrate that the proposed IML-AICE detector consistently outperforms existing trained and blind detection schemes across a range of signal-to-noise ratios and system configurations at low computational complexity.

Received on 03 April 2026; accepted on 07 June 2026; published on 11 June 2026

Keywords: Blind detection, ML detector, Least-Squares, MIMO Systems, Orthogonal Space-Time Block Code

doi:10.4108/eetinis.132.12472

1. Introduction

Space-Time Block Coding is a well-known technique to combat fading in wireless multiple-input multiple-output (MIMO) systems. Among various space-time block codes (STBCs), orthogonal STBCs (OSTBCs) [3–8] are the most attractive because they offer full diversity and enable simple linear maximum-likelihood (ML) detection when perfect channel state information (CSI) is available at the receiver. Consequently, OSTBCs have been extensively studied for reliable wireless communications.

Despite these advantages, OSTBC performance strongly depends on accurate CSI, which is typically obtained through pilot-assisted channel estimation. However, pilot transmission reduces spectral efficiency, particularly in MIMO systems with multiple transmit antennas that require estimating a larger num-ber of channel coefficients. This issue becomes more pronounced in fast time-varying channels with short coherence intervals, where frequent pilot transmission is required to maintain channel estimation accuracy, thereby reducing the effective data rate.

To overcome the limitations of pilot-assisted schemes, blind and semi-blind detection methods have attracted considerable research attention [1, 2, 9–18]. By exploiting the algebraic structure of OSTBCs and the statistical properties of received signals, blind detection techniques can jointly estimate transmitted symbols and channel information without requiring dedicated pilot signals, thereby improving spectral efficiency.

One approach to blind detection of OSTBCs involves first blindly estimating the channel matrices. These estimated channel matrices are then used in a detector, either a coherent ML detector or a sub-optimal

*Corresponding author. Email: tuanlm@ptit.edu.vn

alternative, to recover the transmitted data symbols [9–12]. In [9] and [10], blind channel estimates are obtained from the noise subspace via the singular value decomposition (SVD) of the received signal matrix. By exploiting specific properties of OSTBCs, the authors in [11] developed a method of blindly estimating blind MIMO channel in a closed form. However, the approach in [11] is not applicable to some OSTBCs, including the Alamouti OSTB code, the real OSTBC or the rate-$\frac{1}{2}$ complex OSTBC for four transmit antennas, due to channel nonidentifiability unless a pre-coder is used at the transmitter.

Another way of blind detection is to simultaneously equalize the channel and recover data symbols without explicitly estimating the channel matrix. In [1] and [13], blind and semi-blind detection algorithms were implemented by minimizing the ML metric with respect to the channel matrix and transmitted symbols in an iterative fashion, resulting in the so-called iterative ML. The iterative ML has a low computational load. Unfortunately, it could hardly converge to the global solution in the case of blind detection due to poor initialization. In [2, 14–16], different blind and semi-blind detectors based on the semidefinite relaxation (SDR) and the sphere decoder (SD) were proposed for OSTBCs. It was shown that these decoders noticeably outperform the iterative ML regarding the bit error rate (BER). Nevertheless, the SDR-based detector is only applicable to the Binary-Phase-Shift-Keying (BPSK) and Quadrature-Phase-Shift-Keying (QPSK) constellations. Although the SD is able to work with any phase-shift-keying (PSK) constellations, it fails to provide optimal solutions for QAM constellations [16]. Another drawback of the SDR-based detector and the SD decoder is that their computational loads are much higher than that of the iterative ML, especially when the signal-to-noise ratio (SNR) is small or medium. In [17], blind detection of full-rate STBCs based on linear programming (LP) was presented. By exploiting the implicit structure of STBCs with QAM constellations, the authors are able to cast the problem as linear programming and solve it efficiently. It was shown in [17] that the LP-based detectors are able to work with full-rate STBCs, e.g., the Alamouti code and the quasi-orthogonal space-time code, and converge to global solutions. Nevertheless, they require a large frame length, i.e., more than a hundred codewords per frame, to provide low BER. Furthermore, they are unable to blindly detect STBCs with PSK constellations. In [18], other blind algorithms, which are designated iterative least-squares (ILS) and enhanced ILS (E-ILS), were introduced without requiring any pilot symbols.

A primary problem facing all blind detectors is the identifiability of the OSTBCs inherent in the blind detection of OSTBCs. It was shown in [19, 20] that OSTBCs can be classified into three main categories, namely, *rotatable* OSTBCs, *non-rotatable* OSTBCs, and *strictly non-rotatable* OSTBCs. Among the categories, rotatable OSTBCs suffer from symbol ambiguity effects because a blind receiver can never uniquely identify them up to a sign (U2S). A typical example of rotatable OSTBCs is the OSTBC for two transmit antennas, i.e., the famous Alamouti OSTBC [20]. The non-rotatable OSTBCs can be uniquely identified U2S with a certainty of 100% under the assumption that the frame length is adequately enormous. In contrast, the strictly non-rotatable OSTBCs enable a blind receiver to surely achieve unique blind symbol identification without any assumptions on the data. Typical examples of strictly non-rotatable OSTBCs are real OSTBCs that transmit an odd number of symbols. Interestingly, the authors in [20] devised a subclass of the strictly non-rotatable OSTBCs, termed the *nonintersecting subspace* (NIS) OSTBCs, that experience unique blind symbol identification for any nonzero channel, yet at the cost of some reductions in transmission rates.

In [12], the authors presented a direct channel estimation scheme having a closed-form solution without requiring training data. It was shown that for the real OSTBCs, if the symbol order n is odd, then the channel matrix can be uniquely identified up to a complex scalar. Furthermore, if n is even and the number of transmit antennas is odd, any channel matrix with full column rank is of unique identifiability up to a complex scalar. In [21], the blind identifiability of OSTBCs from the second-order statistics of MIMO channels was investigated. Similar to [12], it was shown in [21] that real OSTBCs with an odd number of symbols allow the MIMO channel to be blindly identified for any number of receive antennas. In addition, any real OSTBC with an odd number of transmit antennas is identifiable, which confirms some of the results in [20] regardless of the finite alphabet constraint. Particularly, the Alamouti code and the real full-rate OSTBC with four transmit antennas are the only nonidentifiable OSTBCs with practical interest. However, to the best of our knowledge, all blind detectors presented in the literature require at least a pilot symbol to completely eliminate sign ambiguity or scalar ambiguity.

In recent years, blind detection based on neural networks has emerged as a promising research direction. In [23], a neural network machine learning (NNML) channel estimator with transmit power-sharing was proposed to enable blind channel estimation for the uncoded space-time labeling diversity (USTLD) system and to minimize channel estimation bandwidth utilization. The blind NNML channel estimator with transmit power-sharing was shown to use only 20% of the bandwidth required by LS and MMSE channel estimators to achieve the same BER performance for the

USTLD system using 16-QAM and 16-PSK modulation schemes.

A closer examination of the approach presented in [23] reveals that the system still requires the transmitter to send pilot symbols. Consequently, the NNML channel estimator in [23] is, in fact, a semi-blind channel estimator. Another limitation of the method lies in its sensitivity to MIMO configurations: for instance, a change in the number of receive antennas may necessitate a new model architecture and re-training of the NNML channel estimation network.

In [24], a one-shot self-supervised learning framework for channel estimation in MIMO systems was developed. The proposed framework consists of a traditional channel estimation module and a denoising module. The number of samples required for offline training is small, and Kang's approach can be directly deployed to adapt to varying channel conditions. Simulation results show that the performance of the one-shot self-supervised learning method is very close to that of the supervised learning approach, while offering improved generalization across different channel environments. However, the method requires pilot symbols for initial rough channel estimation before passing the results to the denoising neural network (NN) for final channel refinement. Clearly, this does not constitute a blind channel estimation method.

The feasibility of pilotless transmission in MIMO systems has recently attracted increasing attention. In [25], machine learning-based pilotless spatial multiplexing was investigated, where jointly trained transmitter and receiver structures enabled blind signal separation and detection without requiring pilot-based channel estimation. Pilotless transmission schemes have also been investigated for massive MIMO uplink systems [26]. More recently, experimental studies have further demonstrated the practical feasibility of deep learning- and AI-based pilotless transmission in wireless MIMO systems [27, 28]. Nevertheless, practical blind OSTBC detection still faces important challenges, including rotational ambiguity and sensitivity to channel initialization, motivating the development of reliable fully blind detection frameworks for OSTBC systems.

In this paper, we investigate the problem of fully blind OSTBC detection in MIMO systems, where neither pilot symbols nor prior channel state information (CSI) are available at the receiver. Unlike pilot-assisted schemes, which incur spectral-efficiency loss due to training overhead, the proposed framework jointly estimates the MIMO channel and recovers transmitted symbols without requiring dedicated pilot signaling. This issue becomes particularly important for OSTBCs with a large number of transmit antennas, whose achievable transmission rates are inherently limited. Specifically, for even n_T, the transmission rate of complex OSTBCs is upper bounded by $\frac{n_T/2+1}{n_T}$ [6], making pilot overhead increasingly detrimental to spectral efficiency as n_T grows.

Despite extensive research on blind OSTBC detection, existing methods still face important challenges, including rotational ambiguity, sensitivity to channel initialization, and limited applicability to certain OSTBC configurations. To address these limitations, we propose a new fully blind detection framework that combines a structurally constrained QAM constellation with an iterative maximum-likelihood detector employing an averaged initial channel estimate (IML-AICE).

The proposed constellation design introduces a real-valued offset parameter α into conventional QAM constellations to suppress the rotational ambiguity considered in the blind OSTBC detection framework with a prescribed confidence level, while keeping the resulting SNR degradation bounded. Based on the resulting structurally constrained constellation, the proposed IML-AICE detector first generates an initial channel estimate by averaging received signal matrices over a frame of Q OSTBC codewords, followed by iterative symbol detection and channel refinement using a cyclic ML procedure. Compared with conventional cyclic ML-based methods, the proposed averaging-based initialization is designed to provide a more reliable initial channel estimate for iterative blind detection while preserving low computational complexity.

In summary, the main contributions of this paper are as follows:

- *Novel ambiguity-suppressing constellation design:* A structurally constrained QAM constellation is proposed to suppress the rotational ambiguity considered in blind OSTBC detection with a prescribed confidence level. Analytical bounds on the offset parameter α are derived to balance ambiguity suppression and performance loss while maintaining bounded SNR degradation.

- *A fully blind low-complexity IML-AICE detector:* A new iterative maximum-likelihood detector with an averaged initial channel estimate is developed to jointly estimate the MIMO channel and recover transmitted symbols without requiring pilot signaling. The proposed detector employs an averaging-based initialization strategy to provide a reliable initial channel estimate for iterative blind detection while preserving low computational complexity.

- *Theoretical performance analysis:* The proposed framework is analytically shown to incur a worst-case SNR loss bounded by approximately 3 dB

relative to coherent ML detection, yielding performance comparable to differential unitary space–time modulation (DUSTM) [22] while being capable of achieving higher spectral efficiency through the use of higher-order QAM constellations.

- *Comprehensive performance validation:* Simulation results demonstrate that the proposed detector achieves superior BER performance to existing trained and semi-blind schemes in [1] over a wide range of SNRs and system configurations, while maintaining significantly lower computational complexity.

The rest of the paper is organized as follows. Section 2 presents a background review of the Clairvoyant ML detector and the blind ML detection of OSTBCs. In Section 3, the structurally constrained constellations are introduced, along with the derivations of the optimized parameters and the initial channel estimates. Section 4 describes the proposed IML-AICE detector. Section 5 provides simulation results and discussions related to the BER performance of different detectors. Finally, Section 6 concludes the paper.

Notation: Bold lowercase and capital letters denote column vectors and matrices, respectively. $\Re\mathfrak{e}(\mathbf{A})$ and $\mathfrak{Im}(\mathbf{A})$ denote the real and imaginary parts of the complex matrix $\mathbf{A}$, respectively. j represents the imaginary unit. $(\cdot)^H$, $(\cdot)^T$, and $(\cdot)^*$ denote the Hermitian transposition, transposition, and complex conjugation operators, correspondingly. $\|\cdot\|$ represents the Frobenius norm of a matrix or the Euclidean norm of a vector. $|\cdot|$ represents the modulus of a complex number. tr$(\cdot)$ and det$(\cdot)$ indicate the trace and the determinant of a matrix, respectively. $E\{s\}$ indicates the ensemble average of the random variable s.

2. Background

2.1. OSTBC with the complex constellations

Figure 1 illustrates the system model of the considered OSTBC scheme. The input bitstream, $b_1, b_2, \cdots$, is mapped to a set of N_s complex symbols, $\{s_1, s_2, \cdots, s_{N_s}\}$, using an M-QAM constellation with M constellation points, i.e., $s_k \in \Omega$. The constellation Ω is normalized such that the average symbol energy is unity, i.e., $E_s = 1$. The transmitter generates an OSTBC codeword $\mathbf{S} = \sum_{k=1}^{N_s} (\mathbf{A}_k \Re\mathfrak{e}(s_k) + j\mathbf{B}_k \mathfrak{Im}(s_k))$, where the $n_T \times N_t$ matrices $\{\mathbf{A}_k, \mathbf{B}_k\}$ are known as dispersion matrices. The codeword $\mathbf{S}$ is transmitted over a frequency-flat, quasi-static $(n_T \times n_R)$ MIMO channel during N_t time slots, where n_T and n_R denote the numbers of transmit and receive antennas, respectively.

For the complex OSTBCs, the dispersion matrices $\{\mathbf{A}_k, \mathbf{B}_k\}$ must satisfy the following conditions [4]:

$$\mathbf{A}_k\mathbf{A}_k^H = C\mathbf{I}_{n_T},\ \mathbf{B}_k\mathbf{B}_k^H = C\mathbf{I}_{n_T}, \tag{1}$$

$$\mathbf{A}_l\mathbf{A}_k^H = -\mathbf{A}_k\mathbf{A}_l^H,\ \mathbf{B}_l\mathbf{B}_k^H = -\mathbf{B}_k\mathbf{B}_l^H,$$
$$\mathbf{A}_l\mathbf{B}_k^H = \mathbf{B}_k\mathbf{A}_l^H, \text{for } k \neq l, \tag{2}$$

where C is a constant.

According to the above properties, the matrix

$$\mathbf{S} = \sum_{k=1}^{N_s} (\mathbf{A}_k \Re\mathfrak{e}(s_k) + j\mathbf{B}_k \mathfrak{Im}(s_k)) \in \mathbb{C}^{n_T \times N_t} \tag{3}$$

is complex-valued and satisfies the condition:

$$\mathbf{S}\mathbf{S}^H = C\|\mathbf{s}\|^2\mathbf{I}_{n_T}. \tag{4}$$

It is assumed that the channel matrix $\mathbf{H} \in \mathbb{C}^{n_R \times n_T}$ remains constant during the transmission of a codeword. Then, the received signal matrix can be written as

$$\mathbf{Y} = \mathbf{H}\mathbf{S} + \mathbf{V} = \mathbf{H}\left(\sum_{k=1}^{N_s} (\mathbf{A}_k \Re\mathfrak{e}(s_k) + j\mathbf{B}_k \mathfrak{Im}(s_k))\right) + \mathbf{V}, \tag{5}$$

where $\mathbf{V}$ denotes the additive white Gaussian noise (AWGN) matrix, whose elements have zero mean and variance σ_n^2.

Assuming that $\mathbf{H}$ is known to the receiver, the ML decoder searches for $\{s_k\}, k = 1, 2, \ldots, N_s$, (over the constellations) that minimize the following function:

$$\|\mathbf{Y} - \mathbf{H}\mathbf{S}\|^2 = \left\|\mathbf{Y} - \mathbf{H}\left(\sum_{k=1}^{N_s} \mathbf{A}_k \Re\mathfrak{e}\,(s_k) + j\mathbf{B}_k \mathfrak{Im}\,(s_k)\right)\right\|^2. \tag{6}$$

Thanks to the properties of $\{\mathbf{A}_k, \mathbf{B}_k\}$ in (1), we obtain the Clairvoyant ML detector for QAM/PSK constellations as follows [1]:

$$\hat{s}_k = \arg\min_{s_k \in \Omega} |\tilde{s}_k - s_k|^2, \tag{7}$$

where $\tilde{s}_k = \frac{\Re\mathfrak{e}(\mathrm{tr}(\mathbf{Y}^H\mathbf{H}\mathbf{A}_k)) - j\mathfrak{Im}(\mathrm{tr}(\mathbf{Y}^H\mathbf{H}\mathbf{B}_k))}{C\|\mathbf{H}\|^2}$, for $k = 1, \ldots, N_s$.

2.2. Blind detection for the complex constellations

Consider again the scenario, where $\mathbf{H}$ is assumed to be constant over a frame of Q complex OSTBC codewords $(Q > 1)$. Based on (5), the complex system equation for the qth codeword, $q = 1, \cdots, Q$, is given by:

$$\mathbf{Y}_q = \mathbf{H}\mathbf{S}_q + \mathbf{V}_q. \tag{8}$$

Assuming that $\mathbf{V}_q$ and $\mathbf{V}_p$ (for $q \neq p$) are independent of each other, the blind ML detector for the complex

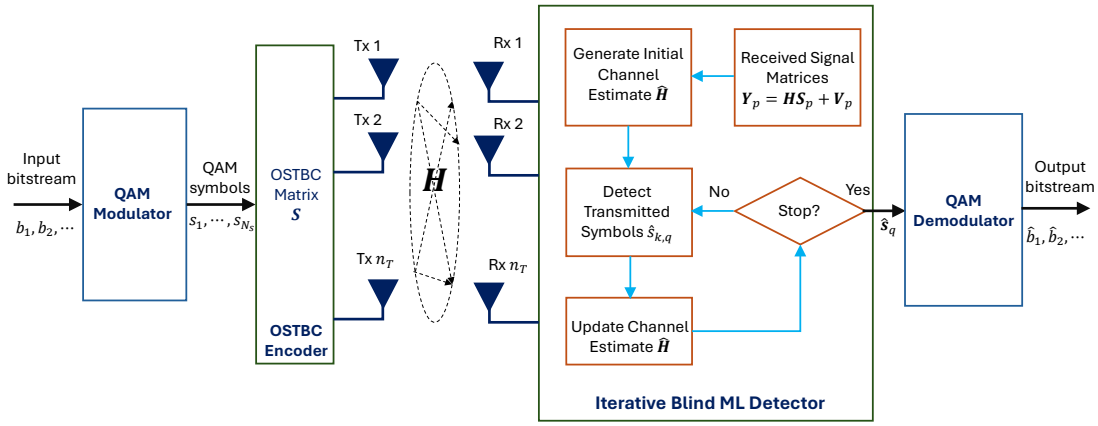

Figure 1. System model of the considered OSTBC scheme with an iterative blind ML detector at the receiver

system is given by [20]:

$$\left\{\hat{\mathbf{H}}, \hat{s}_{k,q}\right\} = \arg \min_{\mathbf{H}, s_{k,q} \in \Omega} \sum_{q=1}^{Q} \left\|\mathbf{Y}_q - \mathbf{H}\mathbf{S}_q\right\|^2, \tag{9}$$

where the unknown $\mathbf{H}$ and $s_{k,q}$ are jointly estimated; $s_{k,p}$ denotes the kth symbol ($k = 1, \ldots, N_s$) in the qth codeword ($q = 1, \ldots, Q$); and

$$\mathbf{S}_q = \sum_{k=1}^{N_s} \mathbf{A}_k \Re\mathfrak{e}\left(s_{k,q}\right) + j\mathbf{B}_k \Im\mathfrak{m}\left(s_{k,q}\right). \tag{10}$$

In the context of OSTBCs, the process of solving the blind detection problem in (9), whether optimally or suboptimally, can be simplified by exploiting the linear dispersion and orthogonal structures of OSTBC codewords discussed above. As introduced in Section I, several algorithms exist to handle (9), including the iterative ML method [1, 13], the closed-form method [11], semidefinite relaxation [2], and sphere decoding [2, 15, 16].

It is important to note, however, that SDR is only applicable to BPSK and QPSK, while sphere decoding performs best with PSK constellations. More importantly, due to their high computational complexity, SDR and sphere decoding are generally impractical for MIMO systems.

For the iterative ML method, an initial estimate of $\mathbf{H}$, i.e, $\hat{\mathbf{H}}$, is obtained using either a pilot codeword or the SVD relaxation method. Then, the detector uses $\hat{\mathbf{H}}$ to recover the transmitted symbols, $\hat{s}_{k,q}$ for $k = 1, \cdots, N_s$ and $q = 1, \cdots, Q$, using (7) with $\mathbf{H} = \hat{\mathbf{H}}$. After that the recovered transmitted symbols $\{\hat{s}_{k,q}\}$ are utilized to re-estimate the channel as follows [1]:

$$\hat{\mathbf{H}} = \frac{\sum_{q=1}^{Q} \mathbf{Y}_q \hat{\mathbf{S}}_q^H}{C \sum_{q=1}^{Q} \|\hat{\mathbf{s}}_q\|^2}, \tag{11}$$

where $\hat{\mathbf{s}}_q = \begin{bmatrix} \hat{s}_{1,q} & \hat{s}_{2,q} & \cdots & \hat{s}_{N_s,q} \end{bmatrix}^T$, and $\hat{\mathbf{S}}_q$ is generated based on (3) with $s_{k,q} = \hat{s}_{k,q}$. The process of alternatively detecting the signals and estimating the channel is repeated until a stopping criterion is satisfied. The resulting qth recovered symbol vector, $\hat{\mathbf{s}}_q$, is passed to the QAM demodulator to generate the corresponding bitstream, as shown in Figure 1. It is worth emphasizing that, due to the use of a small number of pilot symbols as assumed in [1], it is necessary to iteratively refine the channel estimates to improve the accuracy of OSTBC detection. In cases where a large number of pilot symbols is available, accurate channel information can be obtained without the need for iterative refinement.

3. Modification of constellations for blind detection

3.1. Signal ambiguity in blind detection

From (9), we can easily verify that both $\left(\hat{\mathbf{H}}, \hat{\mathbf{S}}_q\right)$ and $\left(-\hat{\mathbf{H}}, -\hat{\mathbf{S}}_q\right)$ are the ML solutions. Moreover, for rotatable OSTBCs, such as the Alamouti OSTBC or the rate-1 real OSTBC for $n_T = 4$ [20], there always exists a matrix $\mathbf{Q}, (\mathbf{Q} \neq \pm\mathbf{I}, \mathbf{Q}^H\mathbf{Q} = \mathbf{Q}\mathbf{Q}^H = \mathbf{I})$ so that $\left(\hat{\mathbf{H}}, \hat{\mathbf{S}}_q\right), \left(\hat{\mathbf{H}}\mathbf{Q}^H, \mathbf{Q}\hat{\mathbf{S}}_q\right)$, and $\left(\hat{\mathbf{H}}\mathbf{Q}, \mathbf{Q}^H\hat{\mathbf{S}}_q\right)$ are all the solutions of (9). It is shown in [20] that the rotation matrix $\mathbf{Q}$, if exists, must be one of the following candidates: $\left\{\pm\mathbf{A}_2\mathbf{A}_1^H, \pm\mathbf{A}_3\mathbf{A}_1^H, \cdots, \pm\mathbf{A}_{N_s}\mathbf{A}_1^H, \pm j\mathbf{B}_1\mathbf{A}_1^H, \pm j\mathbf{B}_2\mathbf{A}_1^H, \cdots, \pm j\mathbf{B}_{N_s}\mathbf{A}_1^H\right\}$.

For instance, consider the Alamouti OSTBC with 16-QAM modulation, i.e., $\Omega = \{s_k, k = 1, 2, \ldots, 16\}$, where the real and imaginary parts of s_k take values from the set $\{\pm\frac{1}{\sqrt{10}}, \pm\frac{3}{\sqrt{10}}\}$.

Let us define $\mathbf{Q} = j\mathbf{B}_2\mathbf{A}_1^H = \begin{bmatrix} 0 & j \\ j & 0 \end{bmatrix}$. We can write:

$$\mathbf{Q}\frac{1}{\sqrt{10}}\begin{bmatrix} -3-j & 1-j \\ -1-j & -3+j \end{bmatrix} = \frac{1}{\sqrt{10}}\begin{bmatrix} 1-j & -1-j3 \\ 1-j3 & 1+j \end{bmatrix}. \tag{12}$$

Equation (12) clearly indicates that both signal vectors $\mathbf{s} = \frac{1}{\sqrt{10}}[-3-j, -1-j]^T$ and $\tilde{\mathbf{s}} = \frac{1}{\sqrt{10}}[1-j, 1-j3]^T$, $\tilde{\mathbf{s}} \neq \pm\mathbf{s}$, can be the solutions of the blind detection problem in (9).

It is evident that, in order to blindly detect OSTBCs without pilot signals, the rotatability of OSTBCs and signal ambiguity must be addressed. In [16], the authors proposed the dual-constellation and superimposed pilot schemes. Nevertheless, the dual-constellation approach sacrifices transmission rate due to the use of lower modulation orders. Moreover, it incurs a 4-dB loss in SNR compared with the training-based detector at a BER of 10^{-3}.

Although the superimposed pilot scheme performs better than the dual-constellation method, it still suffers from approximately a 2.5-dB SNR loss relative to the training-based detector at the same BER. Another important point is that both schemes rely on sphere decoding and are only applicable to PSK constellations.

To deal with the aforementioned issues, we propose to modify the conventional constellations and derive necessary conditions so that signal ambiguity can be eliminated without incurring large performance losses.

3.2. Modification of transmit constellations

Instead of using the conventional constellation for signal transmission, we propose a structurally constrained M-QAM constellation, denoted by Ω_m, where the subscript m indicates *modified*. The proposed constellation is constructed based on the conventional M-QAM constellation as follows:

$$\Omega_m = \left\{ \frac{s_k + \alpha}{\gamma_m} : s_k \in \Omega, k = 1, \cdots, M \right\}, \tag{13}$$

where α is a real number and $\gamma_m = \sqrt{\frac{1}{M}\sum_{k=1}^{M} |s_k + \alpha|^2} = \sqrt{\alpha^2 + 1}$ is the normalized factor to ensure that the average symbol energy of Ω_m equals unity.

For example: Let s_k be the signal points in the 4-QAM constellation, i.e., $\left\{ s_1 = \frac{-1-j}{\sqrt{2}}; s_2 = \frac{-1+j}{\sqrt{2}}; s_3 = \frac{1-j}{\sqrt{2}}; s_4 = \frac{1+j}{\sqrt{2}} \right\}$. Then, the signal points in the structurally constrained constellation Ω_m are $\left\{ \frac{\frac{-1-j}{\sqrt{2}}+\alpha}{\gamma_m}; \frac{\frac{-1+j}{\sqrt{2}}+\alpha}{\gamma_m}; \frac{\frac{1-j}{\sqrt{2}}+\alpha}{\gamma_m}; \frac{\frac{1+j}{\sqrt{2}}+\alpha}{\gamma_m} \right\}$.

3.3. Upper bound for $|\alpha|$

When a new constellation is constructed based on (13), one can easily verify that the distances between the neighbour signal points decreases as α gets bigger, thereby degrading the system performance in regard to BER. In the worst case, α should be chosen so that the system performance is comparable to that of the DUSTM [22]. In other words, the degradation in the BER performance of Ω_m should be within 3 dB (with respect to the SNR) compared to that of Ω. Consequently, the upper bound for $|\alpha|$ is determined as in Proposition 1.

Proposition 1. *Let Ω denote a standard QAM constellation with unit average symbol energy, and Ω_m its structurally constrained version as defined in (13). For the same modulation order, the SNR loss of an OSTBC employing symbols from Ω_m is bounded by 3 dB relative to that using Ω when $|\alpha| \leq 1$.*

Proof: Consider two neighbour signal points $s_k, s_l \in \Omega$. The Euclidean distance between these two points is equal to $d(s_k, s_l) = |s_k - s_l|$. Using (13), we can write:

$$\begin{aligned} \check{s}_k &= \frac{s_k + \alpha}{\gamma_m} = \frac{s_k + \alpha}{\sqrt{\alpha^2 + 1}}, \\ \check{s}_l &= \frac{s_l + \alpha}{\gamma_m} = \frac{s_l + \alpha}{\sqrt{\alpha^2 + 1}}. \end{aligned} \tag{14}$$

It is certain that $\check{s}_k$ and $\check{s}_l$ are also two neighbour signal points in Ω_m, whose Euclidean distance is defined as $d(\check{s}_k, \check{s}_l) = |\check{s}_k - \check{s}_l|$.

From (14), it follows that:

$$d(\check{s}_k, \check{s}_l) = \frac{|s_k - s_l|}{\sqrt{\alpha^2 + 1}} = \frac{d(s_k, s_l)}{\sqrt{\alpha^2 + 1}}. \tag{15}$$

Equation (15) shows that the distance between two neighboring signal points in Ω_m is reduced by a factor of $\sqrt{\alpha^2 + 1}$ compared to that in Ω, where $d(s_k, s_l)$ denotes the minimum Euclidean distance between neighboring points in the original QAM constellation, i.e., $d(s_k, s_l) = d_{\text{old}}$. Therefore, to ensure an SNR loss within 3 dB, the minimum distance in Ω_m should not be smaller than $d_{\text{old}}/\sqrt{2}$, yielding

$$d(\check{s}_k, \check{s}_l) \geq \frac{d(s_k, s_l)}{\sqrt{2}}, \tag{16}$$

or equivalently $\alpha^2 + 1 \leq 2$, which gives

$$|\alpha| \leq 1. \tag{17}$$

3.4. Lower bound for $|\alpha|$

Assuming that the system employs the structurally constrained constellations to generate a frame of Q complex OSTBC codewords, $\mathbf{S}_q, q = 1, \cdots, Q$, and transmits the signals to the receiver. At the receiver, the received signal matrices are again given by (8). Taking

the average of the Q received signal matrices, we get:

$$\mathbf{E}_Y = \frac{1}{Q}\sum_{q=1}^{Q}\mathbf{Y}_q \tag{18}$$

$$= \mathbf{H}\left(\frac{1}{Q}\sum_{q=1}^{Q}\mathbf{S}_q\right) + \frac{1}{Q}\sum_{q=1}^{Q}\mathbf{V}_q. \tag{19}$$

Let us define:

$$\mathbf{E}_S = \frac{1}{Q}\sum_{q=1}^{Q}\mathbf{S}_q, \tag{20}$$

$$\mathbf{E}_V = \frac{1}{Q}\sum_{q=1}^{Q}\mathbf{V}_q. \tag{21}$$

Equation (19) can be rewritten as:

$$\mathbf{E}_Y = \mathbf{H}\mathbf{E}_S + \mathbf{E}_V. \tag{22}$$

Substituting (10) into (20), and taking the structures of the signal points in the structurally constrained constellations into account, we have:

$$\mathbf{E}_S = \frac{1}{Q}\sum_{q=1}^{Q}\left(\sum_{k=1}^{N_s}\mathbf{A}_k\frac{\left(\Re\mathfrak{e}\left(s_{k,q}\right)+\alpha\right)}{\gamma_m} + j\mathbf{B}_k\frac{\mathrm{Im}\left(s_{k,q}\right)}{\gamma_m}\right)$$

$$= \sum_{k=1}^{N_s}\mathbf{A}_k\zeta_{R,k} + j\mathbf{B}_k\zeta_{I,k}, \tag{23}$$

where $s_{k,q} \in \Omega$, and

$$\zeta_{R,k} = \frac{\alpha}{\gamma_m} + \frac{1}{\gamma_m Q}\sum_{q=1}^{Q}\Re\mathfrak{e}\left(s_{k,q}\right), \tag{24}$$

$$\zeta_{I,k} = \frac{1}{\gamma_m Q}\sum_{q=1}^{Q}\mathrm{Im}\left(s_{k,q}\right). \tag{25}$$

Under the assumptions that $\Re\mathfrak{e}\left(s_{k,q}\right)$ and $\mathrm{Im}\left(s_{k,q}\right)$ are independent and identically distributed (i.i.d.) random variables and that the frame length Q is large enough, $\zeta_{R,k}$ can be shown to approximately follow a normal distribution with mean $\mu_\zeta = \frac{\alpha}{\gamma_m}$ and variance $\sigma_\zeta^2 = \frac{1}{2Q\gamma_m^2}$, i.e., $\zeta_{R,k} \sim \mathcal{N}(\mu_\zeta, \sigma_\zeta^2)$ (see Appendix A).

Equation (23) indicates that $\mathbf{E}_S$ is an OSTBC codeword with transmitted symbols $\zeta_{R,k} + j\zeta_{I,k}$. Therefore, if $\zeta_{R,k} > 0$ or $\zeta_{R,k} < 0$, i.e., $|\zeta_{R,k}| > 0$, with probability 1, then we always have $\mathbf{E}_S \neq -\hat{\mathbf{E}}_S$ and $\mathbf{E}_S \neq \mathbf{Q}\hat{\mathbf{E}}_S$ for any matrix $\mathbf{Q}$ satisfying $\mathbf{Q} \neq \pm\mathbf{I}$ and $\mathbf{Q}^H\mathbf{Q} = \mathbf{Q}\mathbf{Q}^H = \mathbf{I}$. This implies that the signal ambiguity problem is completely resolved.

From Equation (22), the channel matrix $\mathbf{H}$ and the signal matrix $\mathbf{E}_S$ can be blindly recovered as follows:

$$\left\{\hat{\mathbf{H}}, \hat{\mathbf{E}}_S\right\} = \arg\min_{\mathbf{H},\mathbf{E}_S}\|\mathbf{E}_Y - \mathbf{H}\mathbf{E}_S\|^2. \tag{26}$$

If the solution $\left\{\hat{\mathbf{H}}, \hat{\mathbf{E}}_S\right\}$ is obtained and $|\zeta_{R,k}| > 0$ with probability 1, then there is no possibility that $\left(-\hat{\mathbf{H}}, -\hat{\mathbf{E}}_S\right)$, $\left(\hat{\mathbf{H}}\mathbf{Q}^H,\ \mathbf{Q}\hat{\mathbf{E}}_S\right)$, or $\left(\hat{\mathbf{H}}\mathbf{Q},\ \mathbf{Q}^H\hat{\mathbf{E}}_S\right)$ could also be solutions to the blind detection problem in (26). That is, $\left\{\hat{\mathbf{H}}, \hat{\mathbf{E}}_S\right\}$ is the unique solution.

It is noteworthy that $\zeta_{R,k} \sim \mathcal{N}(\mu_\zeta, \sigma_\zeta^2)$. Therefore, the condition $|\zeta_{R,k}| > 0$ with probability 1 can be satisfied if and only if $|\alpha| = \infty$. This contradicts Proposition 1, which states that $|\alpha| \leq 1$. To resolve this contradiction, the condition $|\zeta_{R,k}| > 0$ with probability 1 must be relaxed, thereby leading to a lower bound for $|\alpha|$ as defined in Proposition 2.

Proposition 2. *Let κ_p denote the cutoff corresponding to confidence level p $(0 \leq p \leq 1)$ under the Gaussian approximation of $\zeta_{R,k}$. If the offset parameter α is selected such that $|\alpha| \geq \alpha_L$, where $\alpha_L = \kappa_p/\sqrt{2Q}$, then the condition required to avoid rotational ambiguity, namely $|\zeta_{R,k}| > 0$, holds with confidence level p.*

Proof: See the proof in Appendix B.

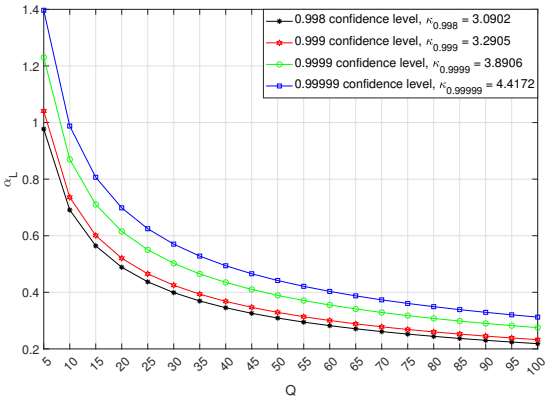

Figure 2. Lower bounds of $|\alpha|$ versus frame length Q for various confidence levels

Illustrated in Fig. 2 are the lower-bound curves, α_L, versus the frame length Q for different confidence levels. It can be observed that, for a given Q, higher confidence l evels r equire l arger v alues o f α_L, whereas for a given confidence l evel p, a s horter f rame length requires a larger value of α_L.

For example, let $Q = 15$. To ensure that $|\zeta_{R,k}| > 0$ holds with confidence l evel $p = 0.99999$, t he offset parameter should satisfy $\alpha \geq \alpha_L = \kappa_{0.99999}/\sqrt{2Q} = 4.4172/\sqrt{30} = 0.8065$. If α is instead selected as $\kappa_{0.998}/\sqrt{2Q} = 3.0902/\sqrt{30} = 0.5642$, then the confidence level decreases to $p = 0.998$.

As shown in (15), the distance between two neighboring signal points in the structurally constrained constellation Ω_m is reduced by a factor of $\sqrt{\alpha^2+1}$ compared to that in the original constellation Ω. Moreover, the SNR

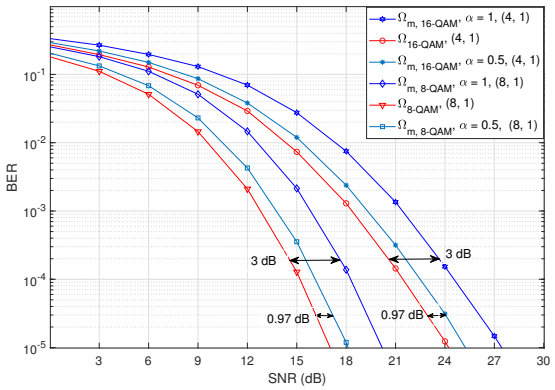

Figure 3. BER curves of the rate-3/4 OSTBC with symbols carved from $\Omega_{16\text{-QAM}}$ and $\Omega_{m,16\text{-QAM}}$ in a (4, 1) system, and those of the rate-1/2 OSTBC with symbols carved from $\Omega_{8\text{-QAM}}$ and $\Omega_{m,8\text{-QAM}}$ in a (8, 1) system. Results are shown for the ML detector with perfect CSI; $\alpha = 0.5$ and $\alpha = 1$

is proportional to the square of the minimum distance between neighboring signal points, i.e., SNR $\propto d^2_{\min}$. Therefore, the system using the structurally constrained constellation incurs an SNR loss of $10\log_{10}\left(\alpha^2+1\right)$ dB compared to the system using the original constellation.

Based on Propositions 1 and 2, the offset parameter α should be selected within the range $\alpha_L \le |\alpha| \le 1$, where $\alpha_L = \kappa_p/\sqrt{2Q}$. Specifically, the lower bound α_L ensures that the condition $|\zeta_{R,k}| > 0$ holds with confidence level p, thereby suppressing the rotational ambiguity considered in the proposed blind OSTBC detection framework. Meanwhile, the upper bound $|\alpha| \le 1$ guarantees that the resulting SNR degradation remains bounded by 3 dB. Under these conditions, the proposed structurally constrained constellation achieves a practical trade-off between ambiguity suppression and performance loss. The corresponding SNR degradation ranges from $10\log_{10}(\alpha_L^2+1)$ dB to a maximum of 3 dB, regardless of modulation order, OSTBC structure, or antenna configuration.

Figure 3 shows the BER curves of a rate-3/4 OSTBC with symbols carved from both the conventional 16-QAM constellation, $\Omega_{16\text{-QAM}}$, and the structurally constrained constellation, $\Omega_{m,16\text{-QAM}}$, in a MIMO system with $n_T = 4$ and $n_R = 1$, referred to as a (4,1) system. It also includes the BER curves of a rate-1/2 OSTBC with symbols carved from the conventional 8-QAM constellation, $\Omega_{8\text{-QAM}}$, and the structurally constrained one, $\Omega_{m,8\text{-QAM}}$, in a (8,1) system. The parameters of the structurally constrained constellations are $\alpha = 0.5$ and $\alpha = 1$.

All systems utilize the clairvoyant ML detector with perfect CSI at the receiver. As observed from Fig. 3, when $\alpha = 1$, using the structurally constrained constellations $\Omega_{m,16\text{-QAM}}$ and $\Omega_{m,8\text{-QAM}}$ results in an SNR loss of 3 dB compared to using the conventional constellations. However, this loss decreases to approximately 0.97 dB when $\alpha = 0.5$. Thus, when selecting α such that $0.5 \le |\alpha| \le 1.0$, the performance loss ranges between 0.97 dB and 3 dB.

4. Proposed IML-AICE detector

In this section, we propose a novel detector, referred to as the iterative maximum-likelihood with averaged initial channel estimate (IML-AICE) detector. The proposed approach leverages (i) structurally constrained constellations, (ii) a newly developed channel estimation method, and (iii) an iterative maximum-likelihood mechanism to jointly perform blind symbol detection and channel estimation without relying on pilot symbols.

4.1. New channel estimate

From (23) and (24) we can write:

$$\mathbf{E}_S = \mathbf{\Gamma} + \bar{\mathbf{E}}_S, \tag{27}$$

where

$$\mathbf{\Gamma} = \sum_{k=1}^{N_s} \mathbf{A}_k \frac{\alpha}{\gamma_m} = \sum_{k=1}^{N_s} \mathbf{A}_k \frac{\alpha}{\sqrt{1+\alpha^2}}, \tag{28}$$

$$\begin{aligned}\bar{\mathbf{E}}_S &= \sum_{k=1}^{N_s} \mathbf{A}_k \left(\zeta_{R,k} - \frac{\alpha}{\gamma_m}\right) + j\mathbf{B}_k\zeta_{I,k} \\ &= \sum_{k=1}^{N_s} \mathbf{A}_k z_{R,k} + j\mathbf{B}_k z_{I,k},\end{aligned} \tag{29}$$

$z_{R,k}$ and $z_{I,k}$ are respectively defined in (A.7) and (A.8) of Appendix A.

It is visible from (28) and (29) that $\mathbf{\Gamma}$ is a real OSTBC constructed based on the set of dispersion matrices $\{\mathbf{A}_k\}$ and the $N_s \times 1$ signal vector $\boldsymbol{\alpha} = \frac{1}{\gamma_m}\begin{bmatrix}\alpha & \alpha & \cdots & \alpha\end{bmatrix}^T$, whereas $\bar{\mathbf{E}}_S$ is a complex OSTBC constructed using $\{\mathbf{A}_k\}, \{\mathbf{B}_k\}, z_{R,k}$, and $z_{I,k}$, for $k = 1, \cdots, N_s$.

From (22) and (27), it follows that:

$$\mathbf{E}_Y = \mathbf{H}\mathbf{\Gamma} + \mathbf{H}\bar{\mathbf{E}}_S + \mathbf{E}_V. \tag{30}$$

Multiplying both sides of (30) by $\mathbf{E}_S^H = \left(\mathbf{\Gamma} + \bar{\mathbf{E}}_S\right)^H$, we get:

$$\begin{aligned}\mathbf{E}_Y\mathbf{E}_S^H &= \left(\mathbf{H}\mathbf{\Gamma} + \mathbf{H}\bar{\mathbf{E}}_S + \mathbf{E}_V\right)\left(\mathbf{\Gamma} + \bar{\mathbf{E}}_S\right)^H \\ &= \mathbf{H}\left(\mathbf{\Gamma}\mathbf{\Gamma}^H + \bar{\mathbf{E}}_S\bar{\mathbf{E}}_S^H\right) + \mathbf{N}_{ES},\end{aligned} \tag{31}$$

where $\mathbf{N}_{ES} = \mathbf{H}\left(\mathbf{\Gamma}\bar{\mathbf{E}}_S^H + \bar{\mathbf{E}}_S\mathbf{\Gamma}^H\right) + \mathbf{E}_V\left(\mathbf{\Gamma} + \bar{\mathbf{E}}_S\right)^H$ is considered as the noise matrix.

It is straightforward to verify that:

$$\mathbf{\Gamma}\mathbf{\Gamma}^H = CN_s\left(\frac{\alpha}{\gamma_m}\right)^2\mathbf{I}_{n_T}, \tag{32}$$

and

$$\bar{\mathbf{E}}_S\bar{\mathbf{E}}_S^H = C\left(\sum_{k=1}^{N_s}\left(z_{R,k}^2 + z_{I,k}^2\right)\right)\mathbf{I}_{n_T}. \tag{33}$$

For OSTBCs with large N_s, e.g., $N_s \geq 4$, (33) can be approximately computed as:

$$\begin{aligned}\bar{\mathbf{E}}_S\bar{\mathbf{E}}_S^H &\approx 2CN_s\left[\frac{1}{2N_s}\sum_{k=1}^{2N_s} z_{R,k}^2\right]\mathbf{I}_{n_T}\\ &\approx 2CN_sE\left\{z_{R,k}^2\right\}\mathbf{I}_{n_T} = \frac{CN_s}{Q\gamma_m^2}\mathbf{I}_{n_T}.\end{aligned} \tag{34}$$

Because $\bar{\mathbf{E}}_S$ is unknown, $\mathbf{E}_S$ is also unknown by the receiver. Fortunately, based on (28), (32), and (34), the receiver can initially compute $\bar{\mathbf{E}}_S$ as:

$$\bar{\mathbf{E}}_S = \left(\sum_{k=1}^{N_s}\mathbf{A}_k\frac{1}{\gamma_m\sqrt{Q}}\right). \tag{35}$$

Under the assumptions that the SNR is considerable and the frame length Q is generously sized, $\mathbf{N}_{ES}$ in (31) can be neglected. Hence, the new channel estimate can be obtained as follows:

$$\hat{\mathbf{H}} = \frac{Q\gamma_m^2}{CN_s\left(\alpha\sqrt{Q}+1\right)^2}\mathbf{E}_Y\hat{\mathbf{E}}_S^H, \tag{36}$$

where

$$\hat{\mathbf{E}}_S = \mathbf{\Gamma} + \bar{\mathbf{E}}_S = \sum_{k=1}^{N_s}\mathbf{A}_k\left(\frac{\alpha}{\gamma_m} + \frac{1}{\gamma_m\sqrt{Q}}\right). \tag{37}$$

Equation (36) clearly proves that by modifying the transmit constellations as in (13), the receiver can effortlessly obtain an initial channel estimate without requiring any pilot symbols.

It is worth noting that the quality of the initial channel estimate in (36) depends on the OSTBC structure, N_s, and Q. The OSTBC orthogonality enables the identities in (32) and (33), thereby suppressing cross terms among symbol components and facilitating channel reconstruction. In addition, when N_s is sufficiently large, e.g., $N_s \geq 4$, the accumulated symbol-energy term in (33) can be approximated by its statistical average as in (34), resulting in a more stable initial channel estimate. Furthermore, increasing Q improves the averaging accuracy in (24) and (25), thereby reducing noise effects and improving the accuracy of the approximation for $\bar{\mathbf{E}}_S$ in (35), which in turn improves the reliability of $\hat{\mathbf{H}}$ in (36). However, a large Q is generally feasible only in slow-fading channels and increases detection delay.

Algorithm 1 IML-AICE Detection Algorithm

Require: Parameter α, N_i, $\left\{\mathbf{Y}_q\right\}_{q=1}^{Q}$, $\{\mathbf{A}_k, \mathbf{B}_k\}_{k=1}^{N_s}$, the structurally constrained transmit constellation Ω_m with M signal points, maximum iterations N_i.
Ensure: Detected transmitted symbols $\hat{s}_{k,q}$ for $k = 1, \cdots, N_s$ and $q = 1, \cdots, Q$.
1: **Initialization:**
2: Generate the matrix $\hat{\mathbf{E}}_S$ as in (37).
3: Compute the averaged signal matrix $\mathbf{E}_Y$ as in (18).
4: Generate the initial channel estimate $\hat{\mathbf{H}}$ based on (36).
5: Assign $\check{s}_{k,q} := 0$ for $k = 1, \cdots, N_s$ and $q = 1, \cdots, Q$.
6: Set iteration counter $i := 1$.
7: **while** $i \leq N_i$ **do**
8: Use $\hat{\mathbf{H}}$ to detect transmitted symbols $\hat{s}_{k,q}$ as in (38).
9: **if** $\hat{s}_{k,q} = \check{s}_{k,q}$ for all k, q **then**
10: **break**.
11: **else**
12: Assign $\check{s}_{k,q} := \hat{s}_{k,q}$.
13: Update channel estimate $\hat{\mathbf{H}}$ as in (11).
14: Increment iteration counter $i := i + 1$.
15: **end if**
16: **end while**
17: **Output:** $\hat{s}_{k,q}$ for $k = 1, \cdots, N_s$ and $q = 1, \cdots, Q$.

4.2. Proposed IML-AICE detector

Given that the system employs a structurally constrained constellation Ω_m, the proposed IML-AICE detector works as follows. First, it computes the average of the Q received signal matrices as in (18). Second, it uses the matrix $\hat{\mathbf{E}}_S$ in (37) to generate an initial channel estimate as in (36). Third, by assuming that $\hat{\mathbf{H}}$ is the correct channel matrix, it detects the transmitted symbols of the qth codewords as follows:

$$\hat{s}_{k,q} = \arg\min_{s_k\in\Omega_m}\left|\tilde{s}_{k,q} - s_k\right|^2, \tag{38}$$

where $\tilde{s}_{k,q} = \frac{\Re\mathfrak{e}\left(\mathrm{tr}\left(\mathbf{Y}^H\hat{\mathbf{H}}\mathbf{A}_k\right)\right) - j\Im\mathfrak{m}\left(\mathrm{tr}\left(\mathbf{Y}^H\hat{\mathbf{H}}\mathbf{B}_k\right)\right)}{C\|\hat{\mathbf{H}}\|^2}$. Fourth, it adopts the detected symbols $\hat{s}_{k,q}$, for $k = 1, \cdots, N_s$, $q = 1, \cdots, Q$, to re-estimate the channel using (11). In the subsequent steps, the proposed IML-AICE detector repeatedly recovers the symbols $\hat{s}_{k,q}$ using (38) and re-estimates the channel based on (11) until the recovered signal vectors are unchanged or until the completion of N_i iterations.

The proposed IML-AICE detection algorithm can be summarized as in Algorithm 1.

4.3. Complexity analysis

In this subsection, the complexity per received information bit of the proposed detector is evaluated in

terms of floating-point operations (*flops*) and compared with existing detectors, including the Trained, Semi-Blind, and SD detectors. We evaluate and compare the complexity per received information bit because the proposed decoder requires no pilot symbols, whereas the existing counterparts do. A real addition, multiplication, or division is counted as one flop. A complex multiplication and a complex division require 6 and 11 flops, respectively.

Complexity of the IML-AICE detector. Based on the above assumptions, the complexity of the IML-AICE can be evaluated to be:

$$\begin{aligned} C_{\text{IML}} &= C_{1,\text{IML}} + C_{2,\text{IML}} \\ &= \Big[2n_R N_t Q + 4n_R n_T N_t\Big] \\ &+ 8N_i N_s Q\Big(n_T n_R N_t + n_T N_t^2 + n_T n_R^2\Big) \\ &- N_i\Big[N_s Q\Big(2(N_t^2 + N_t n_T + n_R^2) + 4N_t + 2n_R + 5M + 2\Big) \\ &+ Q\Big(8n_R n_T N_t + 4N_s - 1\Big) + 2\Big] \text{ flops}, \end{aligned} \tag{39}$$

where $C_{1,\text{IML}}$ and $C_{1,\text{IML}}$ are the complexity of the initialization and the while loop, respectively. By removing low-order terms, the complexity of the IML-AICE is approximately equal to:

$$\begin{aligned} C_{\text{IML}} \approx 2N_i N_s Q\,&[N_t n_T(4n_R - 1) \\ &+ (N_t^2 + n_R^2)(4n_T - 1)\Big] \text{ flops}. \end{aligned} \tag{40}$$

For the proposed IML-AICE detector, no pilot codeword is required. This means that the number of information bits per frame is equal to $QN_s \log_2(M)$. Therefore, the complexity per information bit of the IML-AICE detector is given by:

$$\begin{aligned} C_{\text{IML,b}} &= \frac{C_{\text{IML}}}{QN_s \log_2(M)} \\ &\approx \frac{2N_i\Big[N_t n_T(4n_R - 1) + (N_t^2 + n_R^2)(4n_T - 1)\Big]}{\log_2(M)} \text{ flops}. \end{aligned} \tag{41}$$

Complexity of the Trained detector. For the Trained detector, one OSTBC codeword within a frame of Q OSTBC codewords is used as a pilot for channel estimation. Consequently, the number of information bits per frame is $(Q-1)N_s \log_2(M)$. Therefore, the complexity per bit of the Trained detector is given by:

$$\begin{aligned} C_{\text{Tr},b} &= \frac{C_{\text{Tr}}}{(Q-1)N_s \log_2(M)} \\ &\approx \frac{8Qn_T(N_t n_R + N_t^2 + n_R^2)}{(Q-1)\log_2(M)} \text{ flops}. \end{aligned} \tag{42}$$

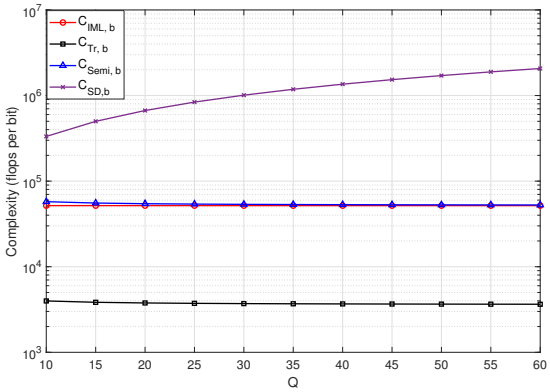

Figure 4. Complexities of the proposed IML-AICE, Trained, Semi-Blind, and SD detectors as functions of Q when detecting rate-1/2 OSTBC in an $(8, 4)$ system. The proposed IML-AICE scheme adopts the structurally constrained 64-QAM constellation, whereas the other detectors utilize the conventional 64-QAM constellation.

Complexity of the Semi-Blind detector. Similar to the Trained detector, the number of information bits per frame for the Semi-Blind detector is $(Q-1)N_s \log_2(M)$. Therefore, the complexity per bit of the Semi-Blind detector is given by:

$$\begin{aligned} C_{\text{Semi,b}} &= \frac{C_{\text{Semi}}}{(Q-1)N_s \log_2(M)} \\ &\approx \frac{2N_i Q}{(Q-1)\log_2(M)}\Big[N_t n_T(4n_R - 1) \\ &+ (N_t^2 + n_R^2)(4n_T - 1)\Big] \text{ flops}. \end{aligned} \tag{43}$$

Complexity of the SD-based detector. Assuming that the SD-based detector operates in the best condition, its total complexity includes the complexity of the preprocessing stage (C_1) and that of the best-case search stage ($C_{\text{SD, best}}$), which is given by:

$$\begin{aligned} C_{\text{SD}} &= C_1 + C_{\text{SD,best}} \\ &\approx \Big[\frac{8}{3}Q^3 N_s^3 + 4Q^2 N_s^2\Big(4n_R N_t^2 + 8n_R^2 N_t + 1\Big) \\ &+ 8N_s^2 N_t^2 n_T\Big] + (2QN_s - 2L_p + 2)^2 \\ &\approx \Big[\frac{8}{3}Q^3 N_s^3 + 4Q^2 N_s^2\Big(4n_R N_t^2 + 8n_R^2 N_t + 2\Big) \\ &+ 8N_s^2 N_t^2 n_T\Big] \text{ flops}. \end{aligned} \tag{44}$$

Unlike the Trained or Semi-Blind detectors, the SD-based detector can operate with just one or two pilot symbols instead of an entire pilot OSTBC codeword. As a result, similar to the case of the proposed IML-AICE detector, we may assume that no pilot codeword is required for the SD-based detector.

Consequently, the number of information bits per frame is given by $QN_s \log_2(M)$. Therefore, the complexity per information bit of the SD-based detector is given by:

$$C_{\mathrm{SD,b}} = \frac{C_{\mathrm{SD}}}{QN_s \log_2(M)} \approx \frac{N_s}{Q \log_2(M)}\left[\frac{8}{3}Q^3 N_s + 4Q^2\left(4n_R N_t^2 + 8n_R^2 N_t + 2\right) + 8N_t^2 n_T\right] \text{flops.} \quad (45)$$

Fig. 4 illustrates the computational complexities per information bit versus the frame length Q for the proposed IML-AICE, Trained, Semi-Blind, and SD detectors when detecting the rate-1/2 OSTBC in an $(8, 4)$ system. The considered rate-1/2 OSTBC for $n_T = 8$ consists of $N_s = 8$ complex symbols transmitted over $N_t = 16$ symbol periods [4]. As can be observed from Fig. 4, the Trained detector exhibits the lowest complexity, followed by the proposed IML-AICE and Semi-Blind detectors, whereas the SD-based detector has the highest complexity and increases rapidly as Q grows. This behavior follows directly from (41)–(43) and (45). For sufficiently large Q, the dominant terms of the total computational complexities of the proposed IML-AICE, Trained, and Semi-Blind detectors scale linearly with Q. Since the total number of transmitted bits is also proportional to Q, their computational complexities per bit become nearly independent of Q. In contrast, the total computational complexity of the SD detector scales cubically with Q according to (45). Therefore, after normalization by the number of transmitted bits, $C_{\mathrm{SD},b}$ still scales proportionally to Q^2, thereby explaining the upward trend observed in Fig. 4.

For example, when Q increases from 20 to 40, $C_{\mathrm{SD},b}$ increases from approximately 6.68×10^5 to 1.36×10^6 flops, whereas $C_{\mathrm{Semi},b}$, $C_{\mathrm{IML},b}$, and $C_{\mathrm{Tr},b}$ vary only slightly around 5.3×10^4, 5.2×10^4, and 3.7×10^3 flops, respectively.

5. Simulation results and discussions

In this section, the BER performance of the proposed IML-AICE detector is evaluated and compared with that of the maximum-likelihood (ML) detector with perfect CSI, as well as the Blind and Semi-Blind detectors in [1]. The SD-based detector is excluded because it does not support QAM-modulated symbols and incurs prohibitively high computational complexity. Unlike the Blind and Semi-Blind detectors, which employ conventional constellations and require pilot-assisted transmission in the Semi-Blind case, the proposed IML-AICE detector operates without pilot signaling using structurally constrained constellations. The rate-$\frac{1}{2}$ OSTBCs for $n_T = 6$ and $n_T = 8$, consisting of $N_s = 8$ complex symbols transmitted over $N_t = 16$ symbol periods, as presented in [4], are considered.

Performance comparisons are made at BER = 10^{-5}. The main simulation parameters are summarized in Table 1.

Table 1. Simulation parameters used for BER performance evaluation

Parameter	$(6, 2)$ **system**	$(8, 4)$ **system**
n_T	6	8
n_R	2	4
OSTBC rate	$\frac{1}{2}$	$\frac{1}{2}$
N_s	8	8
N_t	16	16
Modulation	16-QAM	64-QAM
α	0.5	0.4
Q	15	20
Compared detectors	ML with CSI, Proposed IML-AICE, Blind, and Semi-Blind detectors	
N_i	15	
Stopping criterion	Stop after N_i iterations or when two consecutive recovered frames are identical	

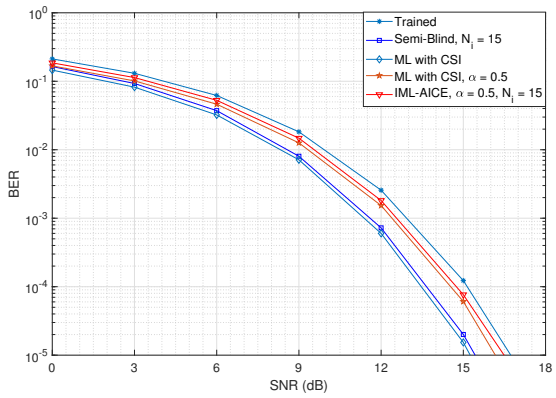

Figure 5. BERs of the rate-$\frac{1}{2}$OSTBC in the $(6, 2)$ system when detected by the proposed IML-AICE and the existing Blind and Semi-Blind detectors. The transmitted symbols are drawn from the conventional 16-QAM and the structurally constrained 16-QAM constellations with $\alpha = 0.5$. Frame length: $Q = 15$

Fig. 5 illustrates the BERs of the rate-$\frac{1}{2}$ OSTBC with symbols drawn from the conventional 16-QAM and the structurally constrained 16-QAM constellations with $\alpha = 0.5$ in the $(6, 2)$ system for the three aforementioned detectors. The BER curves of the ML detector with perfect CSI are also included as benchmarks. Both the Trained and Semi-Blind detectors require one pilot codeword, resulting in a training overhead of $\frac{1}{12} \approx$

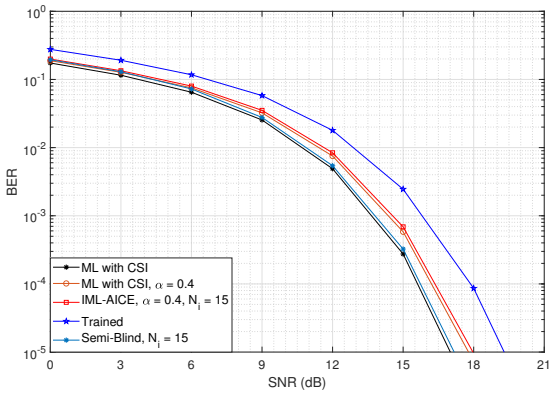

Figure 6. BERs of the rate-$\frac{1}{2}$OSTBC in the (8, 4) system when detected by the proposed IML-AICE and the existing Blind and Semi-Blind detectors. The transmitted symbols are drawn from the conventional 64-QAM and the structurally constrained 64-QAM constellations with $\alpha = 0.4$. Frame length: $Q = 20$

8.3%. This clearly shows that the IML-AICE enables the system to achieve approximately 8.3% improvement in data rate compared to both the Trained and Semi-Blind detectors.

Moreover, as observed in Fig. 5, the IML-AICE approaches the performance of the ML detector with CSI for $\alpha = 0.5$ and outperforms the Trained detector by nearly 0.25 dB in SNR. However, it experiences approximately a 1.0 dB degradation in SNR compared to the Semi-Blind detector. This performance gap is attributed to the use of the structurally constrained 16-QAM with $\alpha = 0.5$, which incurs an SNR loss of $10\log_{10}(1 + 0.5^2) \approx 0.97$ dB relative to the conventional 16-QAM, as confirmed b y t he B ER c urves o f t he ML detector with CSI and with CSI using $\alpha = 0.5$.

Similar results can be observed in Fig. 6, which shows the BERs of the rate-$\frac{1}{2}$ OSTBC with symbols drawn from the conventional 64-QAM and the structurally constrained 64-QAM constellations with $\alpha = 0.4$ in the $(8, 4)$ system. In this scenario, the frame length Q is set to 20. Consequently, the training overhead for the Trained and Semi-Blind detectors is $\frac{1}{20} = 5\%$. This implies that the IML-AICE enables the system to achieve a data rate improvement of 5% over both the Trained and Semi-Blind detectors.

Again, the IML-AICE approaches the performance of the ML detector with CSI for $\alpha = 0.4$. The performance gap between the IML-AICE and the Trained detector increases to nearly 1.25 dB, while the gap between the IML-AICE and the Semi-Blind detector is reduced to approximately 0.8 dB.

The results from Fig. 4, Fig. 5, and Fig. 6 allow us to conclude that the Trained detector has the lowest complexity but suffers from performance degradation and reduced data rate. At the same level of complexity, the IML-AICE enables the system to improve data rate by 5% to 8.3%, albeit at the cost of a performance loss of approximately 0.8 dB to 1.0 dB in SNR. This confirms the inherent trade-off among data rate, performance, and detection complexity in MIMO systems.

6. Conclusion

In this paper, we propose structurally constrained QAM constellations to eliminate the signal ambiguity problem inherent with the blind detection of OSTBCs. Subsequently, we derive an initial channel estimate and incorporated an iterative signal detection mechanism to develop the IML-AICE detector, which enables OSTBCs in MIMO systems to be recovered without relying on any pilot symbols. With the proposed IML-AICE detector, the system can improve its data rate by a factor of $\frac{Q}{Q-1}$, resulting in data rate improvements of approximately 9% and 5% for $Q = 12$ and $Q = 20$, respectively, compared to the Trained and Semi-Blind detectors. Furthermore, simulation results demonstrate that the proposed IML-AICE detector enables blind detection of OSTBCs with symbols drawn from structurally constrained QAM constellations across various MIMO antenna configurations, while achieving performance close to that of the optimal ML decoder under known CSI for the selected values of α.

7. Appendices

Appendix A. Distribution of $\zeta_{R,k}$ and $\zeta_{I,k}$

Let us consider the kth transmitted symbol in the qth codeword, i.e., $s_{k,q}$. If transmitted symbols drawn from Ω are equally likely, then $\Re\mathfrak{e}\left(s_{k,q}\right)$ and $\mathrm{Im}\left(s_{k,q}\right)$ are also equally likely to be transmitted. The means and variances of $\Re\mathfrak{e}\left(s_{k,q}\right)$ and $\mathrm{Im}\left(s_{k,q}\right)$ can be evaluated to be:

$$\mu_{\Re\mathfrak{e}\left(s_{k,q}\right)} = \mu_{\mathrm{Im}\left(s_{k,q}\right)} = E\{\Re\mathfrak{e}\left(s_{k,q}\right)\} = E\{\mathrm{Im}\left(s_{k,q}\right)\} = 0, \tag{A.1}$$

$$\sigma^2_{\Re\mathfrak{e}\left(s_{k,q}\right)} = \sigma^2_{\mathrm{Im}\left(s_{k,q}\right)} = E\{|\Re\mathfrak{e}\left(s_{k,q}\right)|^2\} = \frac{1}{2}. \tag{A.2}$$

The proof for equations (A.1) and (A.2) can be presented as follows. For simplicity, let us consider an M-QAM constellation Ω, where $M = 2^{2n}$ for some integer $n \geq 1$. Since $s_{k,q} \in \Omega$, $\Re\mathfrak{e}\left(s_{k,q}\right)$ and $\mathrm{Im}\left(s_{k,q}\right)$ can be drawn from the set $\mathcal{L} = \left\{\pm\gamma(\sqrt{M}-1), \pm\gamma(\sqrt{M}-3), \cdots, \pm\gamma\right\}$, where $\gamma = \sqrt{\frac{3}{2(M-1)}}$ is the normalized factor, with an equi-probability of $p = 1/\sqrt{M}$. If we define $l = 1, 2, \cdots, \sqrt{M}$, then the corresponding values of $\Re\mathfrak{e}\left(s_{k,q}\right)$ (or, $\mathrm{Im}\left(s_{k,q}\right)$) can be represented as:

$$\Re\mathfrak{e}\left(s_{k,q}(l)\right) = \gamma(2l - (\sqrt{M}+1)). \tag{A.3}$$

The mean of $\Re\mathfrak{e}\left(s_{k,q}\right)$ is evaluated to be:

$$\begin{aligned}\mu_{\Re\mathfrak{e}\left(s_{k,q}\right)} &= E\{\Re\mathfrak{e}\left(s_{k,q}\right)\} = \frac{1}{\sqrt{M}}\sum_{l=1}^{\sqrt{M}}\Re\mathfrak{e}\left(s_{k,q}(l)\right)\\ &= \frac{\gamma}{\sqrt{M}}\sum_{l=1}^{\sqrt{M}}(2l-(\sqrt{M}+1))\\ &= \frac{\gamma}{\sqrt{M}}\left[2\frac{(\sqrt{M}+1)\sqrt{M}}{2}-(\sqrt{M}+1)\sqrt{M}\right]=0.\end{aligned} \tag{A.4}$$

Since $\mu_{\Re\mathfrak{e}\left(s_{k,q}\right)}=0$, the variance of $\Re\mathfrak{e}\left(s_{k,q}\right)$ is evaluated to be:

$$\begin{aligned}\sigma^2_{\Re\mathfrak{e}\left(s_{k,q}\right)} &= E\{\left(\Re\mathfrak{e}\left(s_{k,q}\right)\right)^2\} = \frac{1}{\sqrt{M}}\sum_{l=1}^{\sqrt{M}}\left(\Re\mathfrak{e}\left(s_{k,q}(l)\right)\right)^2\\ &= \frac{\gamma^2}{\sqrt{M}}\sum_{l=1}^{\sqrt{M}}\left(2l-(\sqrt{M}+1)\right)^2\\ &= \frac{4\gamma^2}{\sqrt{M}}\left[\sum_{l=1}^{\sqrt{M}}l^2-\sum_{l=1}^{\sqrt{M}}l(\sqrt{M}+1)+\sum_{l=1}^{\sqrt{M}}\frac{(\sqrt{M}+1)^2}{4}\right].\end{aligned} \tag{A.5}$$

After some tedious manipulation, we get:

$$\begin{aligned}\sigma^2_{\Re\mathfrak{e}\left(s_{k,q}\right)} &= \frac{4\gamma^2}{\sqrt{M}}\left[\frac{\sqrt{M}(M-1)}{12}\right]\\ &= \frac{3}{2(M-1)}\frac{4}{\sqrt{M}}\left[\frac{\sqrt{M}(M-1)}{12}\right]=\frac{1}{2}.\end{aligned} \tag{A.6}$$

Let us define new random variables $z_{R,k}$ and $z_{I,k}$ as follows:

$$z_{R,k} = \frac{1}{\gamma_m Q}\sum_{q=1}^{Q}\Re\mathfrak{e}\left(s_{k,q}\right), \tag{A.7}$$

$$z_{I,k} = \frac{1}{\gamma_m Q}\sum_{q=1}^{Q}\mathfrak{Im}\left(s_{k,q}\right), \tag{A.8}$$

where $\Re\mathfrak{e}\left(s_{k,q}\right)$ and $\mathfrak{Im}\left(s_{k,q}\right)$ are independent and identically distributed (i.i.d.) random variables.

Using the results in (A.1) and (A.2), we can easily obtain the means, $\mu_{z_{R,k}}=E\{z_{R,k}\}$, $\mu_{z_{I,k}}=E\{z_{I,k}\}$, and the variances, $\sigma^2_{z_{R,k}}=E\{|z_{R,k}|^2\}$, $\sigma^2_{z_{I,k}}=E\{|z_{I,k}|^2\}$, of $z_{R,k}$ and $z_{I,k}$ as follows:

$$\mu_{z_{R,k}} = \mu_{z_{I,k}} = \frac{1}{\gamma_m Q}\sum_{q=1}^{Q}E\left\{\Re\mathfrak{e}\left(s_{k,q}\right)\right\}=0, \tag{A.9}$$

$$\sigma^2_{z_{R,k}} = \sigma^2_{z_{I,k}} = \frac{1}{\gamma_m^2 Q^2}\sum_{q=1}^{Q}\sigma^2_{\Re\mathfrak{e}\left(s_{k,q}\right)} = \frac{1}{2Q\gamma_m^2}. \tag{A.10}$$

From (24) we can re-write $\zeta_{R,k}$ as:

$$\zeta_{R,k} = \frac{\alpha}{\gamma_m}+z_{R,k}. \tag{A.11}$$

Thus, it is straightforward to show that $\zeta_{R,k}$ is a random variable with the following mean and variance:

$$\mu_\zeta = \frac{\alpha}{\gamma_m}, \tag{A.12}$$

$$\sigma^2_\zeta = \frac{1}{2Q\gamma_m^2}. \tag{A.13}$$

According to the Central Limit Theorem (CLT), as the frame length Q gets large enough, $\zeta_{R,k}$ approximately follows a normal distribution with mean $\mu_\zeta=\frac{\alpha}{\gamma_m}$ and variance $\sigma^2_\zeta=\frac{1}{2Q\gamma_m^2}$, i.e., $\zeta_{R,k}\sim\mathcal{N}(\mu_\zeta,\sigma^2_\zeta)$, whose probability density function (pdf) is defined by:

$$p(z) = \frac{1}{\sigma_\zeta\sqrt{2\pi}}\exp\left(-\frac{1}{2}\left(\frac{z-\mu_\zeta}{\sigma_\zeta}\right)^2\right). \tag{A.14}$$

Similarly, from (25) it follows that $\zeta_{I,k}\sim\mathcal{N}(0,\sigma^2_\zeta)$.

Appendix B. Proof of Proposition 2

It is well known that for the normal distribution $\zeta_{R,k}\sim\mathcal{N}(\mu_\zeta,\sigma^2_\zeta)$, the confident interval (CI) for the mean is defined as

$$CI = [\mu_\zeta-\kappa_p\sigma_\zeta,\mu_\zeta+\kappa_p\sigma_\zeta], \tag{B.1}$$

where κ_p determines the cutoff points for the p confidence level, where $0\le p\le 1$. In order to have $\zeta_{R,k}>0$ with probability of p, we have to find α so that the lower bound of the p confidence interval in (B.1) is greater than 0, that is:

$$\mu_\zeta-\kappa_p\sigma_\zeta>0. \tag{B.2}$$

Substituting μ_ζ in (A.12) and σ_ζ in (A.13) into (B.2), we get:

$$\frac{\alpha}{\gamma_m}>\frac{\kappa_p}{\gamma_m\sqrt{2Q}}. \tag{B.3}$$

Finally, we have:

$$\alpha>\frac{\kappa_p}{\sqrt{2Q}}. \tag{B.4}$$

Analogously, in order to have $\zeta_{R,k}<0$ with probability of p, we have to find α so that the upper bound of the p confidence interval in (B.1) is smaller than 0, that is:

$$\mu_\zeta+\kappa_p\sigma_\zeta<0. \tag{B.5}$$

After some manipulation, we get:

$$\alpha<-\frac{\kappa_p}{\sqrt{2Q}}. \tag{B.6}$$

In general, α should be selected so that $|\alpha|>\alpha_L$, where $\alpha_L=\frac{\kappa_p}{\sqrt{2Q}}$ is the lower bound for $|\alpha|$, to make $|\zeta_{R,k}|>0$ with the p confidence level.

References

[1] Stoica P, Ganesan G. Space–time block codes: trained, blind, and semi-blind detection. Digit Signal Process. 2003;13(1):93–105.

[2] Ma WK, Vo BN, Davidson TN, Ching PC. Blind ML detection of orthogonal space-time block codes: Efficient high-performance implementations. IEEE Trans Signal Process. 2006;54(2):738–751.

[3] Alamouti SM. A simple transmit diversity technique for wireless communications. IEEE J Sel Areas Commun. 1998;16(8):1451–1458.

[4] Tarokh V, Jafarkhani H, Calderbank AR. Space-time block codes from orthogonal designs. IEEE Trans Inf Theory. 1999;45(5):1456–1467.

[5] Ganesan G, Stoica P. Space-time block codes: A maximum SNR approach. IEEE Trans Inf Theory. 2001;47(4):1650–1656.

[6] Liang XB. Orthogonal designs with maximal rates. IEEE Trans Inf Theory. 2003;49(10):2468–2503.

[7] Su W, Xia XG, Liu KJR. A systematic design of high-rate complex orthogonal space-time block codes. IEEE Commun Lett. 2004;8(6):380–382.

[8] Halmi MH, Abdellatif M, Nooridin N. Orthogonal space-time block codes for large MIMO systems. In: Proc Int Conf Communications, Management and Telecommunications; 2015. p. 78–82.

[9] Zhou S, Muquet B, Giannakis GB. Subspace-based (semi-)blind channel estimation for block precoded space-time OFDM. IEEE Trans Signal Process. 2002;50(5):1215–1228.

[10] Ding Z, Ward DB. Subspace approach to blind and semi-blind channel estimation for space-time block codes. IEEE Trans Wireless Commun. 2005;4(2):357–362.

[11] Shahbazpanahi S, Gershman AB, Manton JH. Closed-form blind MIMO channel estimation for orthogonal space-time block codes. IEEE Trans Signal Process. 2005;53(12):4506–4517.

[12] Ammar N, Ding Z. Channel identifiability under orthogonal space-time coded modulations without training. IEEE Trans Wireless Commun. 2006;5(5):1003–1013.

[13] Larsson EG, Stoica P, Li J. Orthogonal space-time block codes: Maximum likelihood detection for unknown channels and unstructured interferences. IEEE Trans Signal Process. 2003;51(2):362–372.

[14] Ma WK, Ching PC, Davidson TN, Xia XG. Blind maximum-likelihood decoding for orthogonal space-time block codes: A semidefinite relaxation approach. In: Proc IEEE GLOBECOM; 2003. p. 2094–2098.

[15] Le MT, Pham VS, Mai L, Yoon G. Efficient algorithm for blind detection of orthogonal space-time block codes. IEEE Signal Process Lett. 2007;14(5):301–304.

[16] Cui T, Tellambura C. Efficient blind receiver design for orthogonal space-time block codes. IEEE Trans Wireless Commun. 2007;6(5):1890–1899.

[17] Muhammad M, Ding Z. A linear programming receiver for blind detection of full-rate space-time block codes. IEEE Trans Signal Process. 2010;58(11):5819–5834.

[18] Tian X, Li M, Ti G, Liu W. Fast detection of orthogonal space-time block codes with unknown channel. IEEE Commun Lett. 2016;20(9):1896–1899.

[19] Ma WK, Ching PC, Davidson TN, Vo BN. Blind symbol identifiability of orthogonal space-time block codes. In: Proc IEEE ICASSP; 2004. p. iv-821.

[20] Ma WK. Blind ML detection of orthogonal space-time block codes: Identifiability and code construction. IEEE Trans Signal Process. 2007;55(7):3312–3324.

[21] Via J, Santamaria I. On the blind identifiability of orthogonal space-time block codes from second-order statistics. IEEE Trans Inf Theory. 2008;54(2):709–722.

[22] Hochwald BM, Sweldens W. Differential unitary space-time modulation. IEEE Trans Commun. 2000;48(12):2041–2052.

[23] Mthethwa B, Xu H. Deep learning-based wireless channel estimation for MIMO uncoded space-time labeling diversity. IEEE Access. 2020;8:224608–224620.

[24] Kang K, Hu Q, Cai Y, Eldar YC. One-shot learning for channel estimation in massive MIMO systems. In: Proc IEEE VTC-Spring; 2023. p. 1–5.

[25] Korpi D, Honkala M, Huttunen JMJ. Deep learning-based pilotless spatial multiplexing. In: Proc Asilomar Conf Signals, Systems, and Computers; 2023. p. 1025–1029.

[26] Aswathylakshmi P, Ganti RK. Pilotless uplink for massive MIMO systems. In: Proc IEEE Global Communications Conference (GLOBECOM); 2023. p. 4205–4210.

[27] Yamamoto H, et al. Indoor experiments on deep learning-based pilotless transmission scheme. In: Proc IEEE Vehicular Technology Conference (VTC-Fall); 2025. p. 1–5.

[28] Yamamoto H, et al. Indoor experimental trial on AI-based pilotless transmission. IEEE Access. 2026;14:64161–64170.